Figures

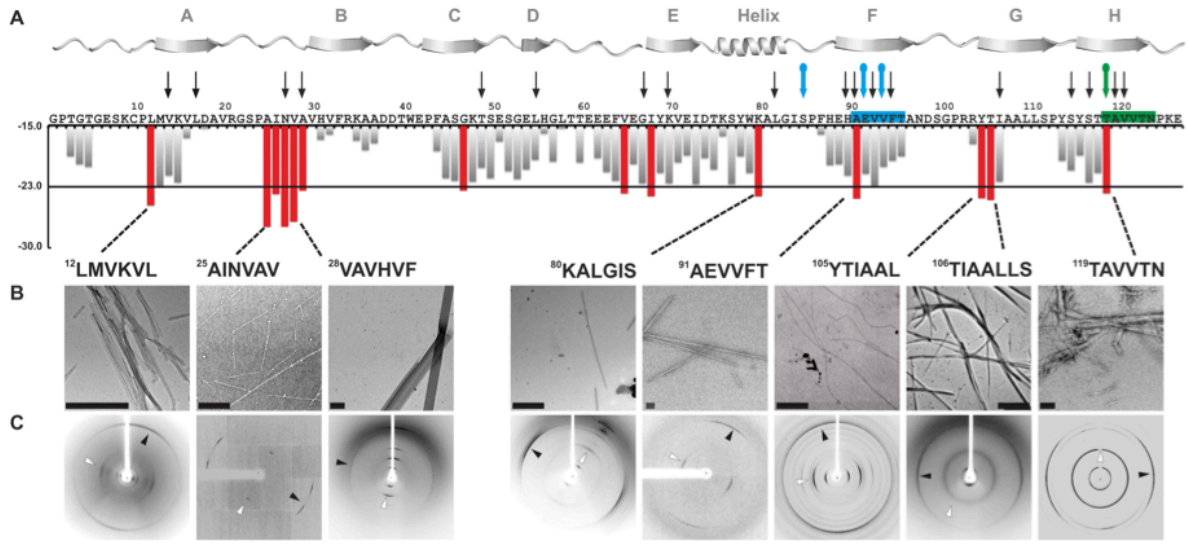

FIGURE 1. Identifying amyloidogenic segments in TTR. A. Propensities of steric zipper formation of each 6-residue segment within the TTR sequence. Computationally predicted segments with steric-zipper propensities are represented with red bars. The cartoon of the secondary structure of native TTR is shown on top of the sequence. Black arrows mark residues where proline replacement did not hinder TTR aggregation. Blue arrows mark proline replacements that hindered TTR aggregation. The green arrow marks the mutation T119M, which protects TTR against fibril formation (Alves et al., 1993). B. TEM micrographs of the fibrils formed after 7 days of incubation (scale bar, 500 nm). C. Amyloid x-ray cross-beta diffraction pattern of the samples containing fibrils shown in B. The arrowheads point to the meridional reflection at 4.7-4.8 Å spacings (parallel to the fibril axis, black arrowheads) and equatorial reflections at ~10 Å spacings (white arrowheads). Notice that all 8 of the examined segments predicted to form amyloid fibrils do in fact form amyloid fibrils.

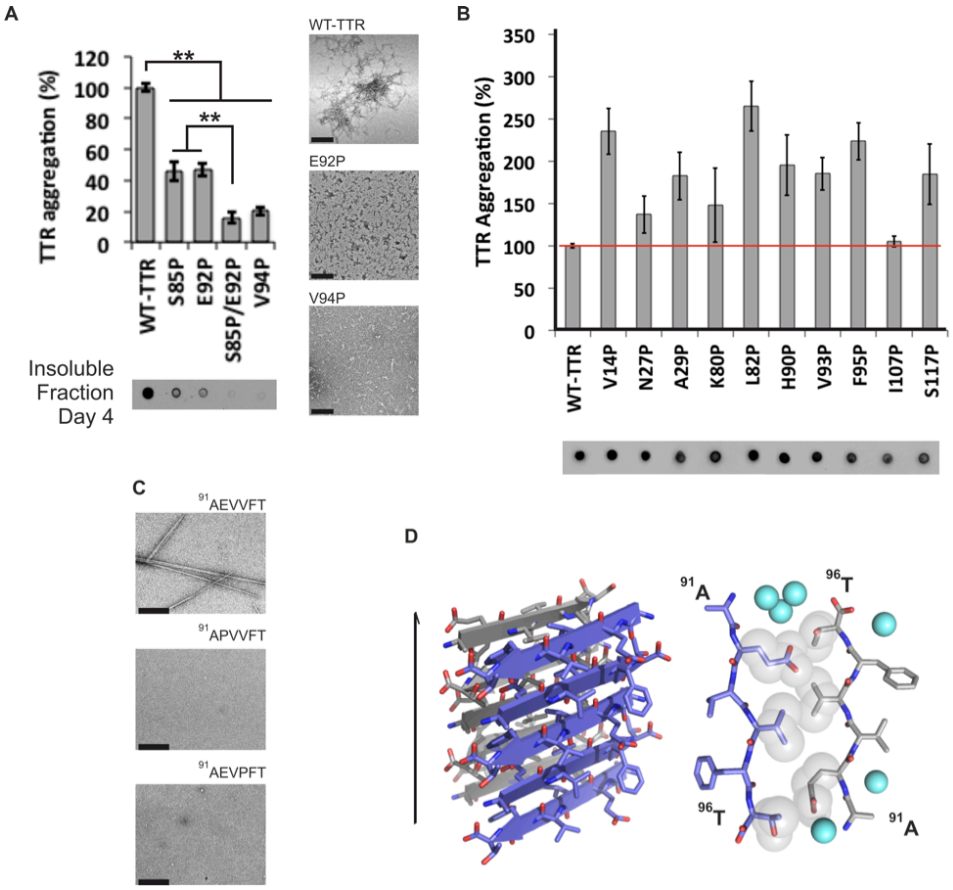

FIGURE 2. Beta-strand F as an aggregation-driving segment in TTR, suitable for aggregation inhibitor design. TTR aggregation of the protein variants that showed significant delay (**A**) and those which did not decrease protein aggregation (**B**). Those TTR proline variants that are not shown were found to be insoluble. Histograms show percentage of TTR aggregation, using WT-TTR to normalize to 100%. The aggregation was measured by absorbance of the samples at 400 nm after 4 days of incubation at 37º C and pH 4.3 with no shaking. The bottom panel shows a His-probe dot blot of the insoluble fraction corresponding to sample above, after solubilization with guanidinium hydrochloride. On the right, TEM micrographs of protein aggregates (scale bar, 100 nm) after 7 days of incubation. Error bars represent SD, ** symbolizes p-value≤0.003, N=3. **C.** TEM micrographs of peptides in isolation after 7 days of incubation in PBS with no shaking (scale bar, 500 nm). **D.** Crystal structure of the segment ^{91}AEVVFT^{96} from beta-strand F, forming a Class-7 steric zipper. One sheet is shown as blue; the other as gray. On the left, a lateral view of the fibril, with the fibril axis shown by the narrow black arrow. On the right, the view is down the fibril axis, showing two beta sheets in projection. Water molecules are shown as aquamarine spheres.

Spheres represent the Van Der Waals radii of the side chain atoms of the tightly packed fibril core.

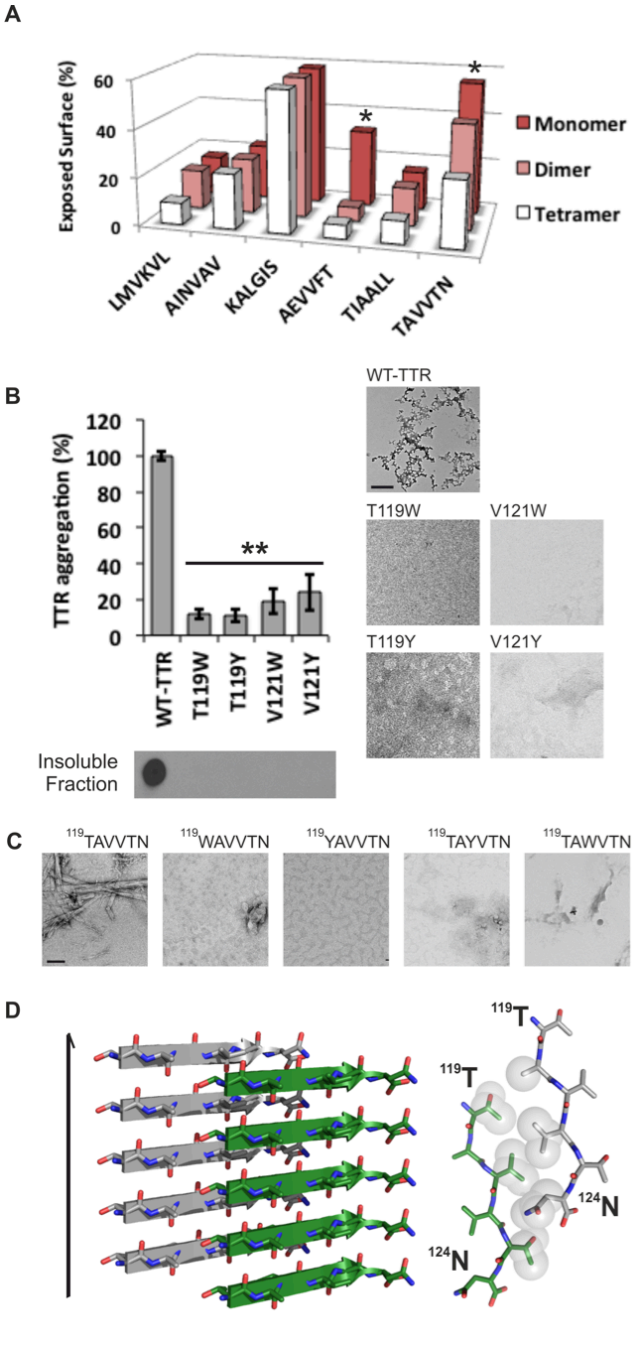

FIGURE 3. Beta-strand H as a second aggregation-driving segment, suitable as a target for aggregation inhibitor design. A. Solvent accessible area of the different segments of TTR was performed by Areaimol using the structure of WT TTR, in three different conformations: tetramer (white), dimer (pink) and monomer (dark pink). The percentage of the solvent accessible area of each segment compared to the total area is shown in this graph. Notice that the segments ^{91}AEVVFT^{96} and ^{119}TAVVTN^{124} (stars) are indeed more exposed when TTR is in a monomeric form. **B.** TTR aggregation of variants with substitutions on the strand H. The histogram on the top shows the percentage of TTR aggregation after 4 days of incubation, measured by absorbance at 400 nm, with WT aggregation normalized to 100%. Below, a His-probe dot blot shows the insoluble fraction of the samples after 4 days of incubation and solubilization with guanidinium hydrochloride. On the bottom panels, TEM images from the samples after 7 days of incubation. This shows that the substitutions of residues T119 and V121 did indeed hinder protein aggregation. Error bars represent SD, ** symbolizes p-value≤0.003, N=3. **C.** TEM micrographs of peptides in isolation after 7 days of incubation in PBS with no shaking (scale bar, 500 nm). **D.** Crystal structure of the segment ^{119}TAVVTN^{124} from the beta-strand H, forming a Class-2

steric zipper. One sheet of the zipper is gray; the other green. On the left, lateral view of the fibril, with the fibril axis indicated by the narrow black arrow. On the right, the view is down the fibril axis, showing two beta sheets in projection. Spheres represent the Van Der Waals radii of the side chain atoms of the tightly packed fibril core.

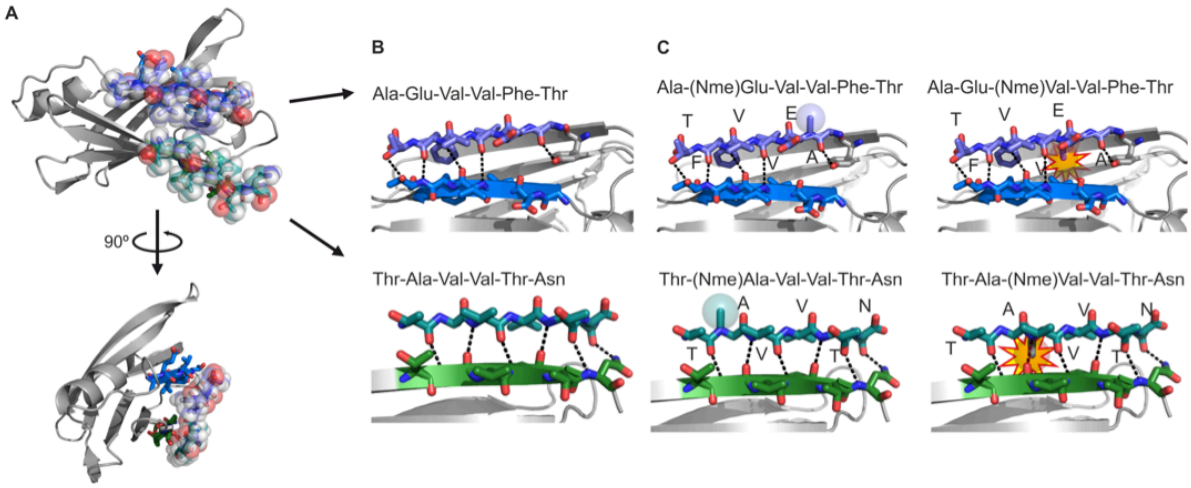

FIGURE 4. Design of sequence-specific peptide inhibitors of TTR aggregation. A. Design of aggregation inhibitors using the TTR monomer as a template. Peptide inhibitors AEVVFT (blue) and TAVVTN (green), are represented as atoms sitting in their designed positions against strands F and H, shown as ribbons as parts of the TTR monomer. **B.** Lateral view of the F and H strands in the docking model between TTR monomer shown as ribbons, and the peptides AEVVFT and TAVVTN, showing the designed pattern of hydrogen bonding (dashed lines). **C.** In order to increase solubility and reduce protease sensitivity, we added N-methylated amino acids to the initial inhibiting peptides. We used the docking model to predict the favorable positions. The colored spheres represent the van der Waals radii of the N-methyl groups in favorable positions; the yellow stars represent the clashing of the N-methyl modifications with the TTR monomer.

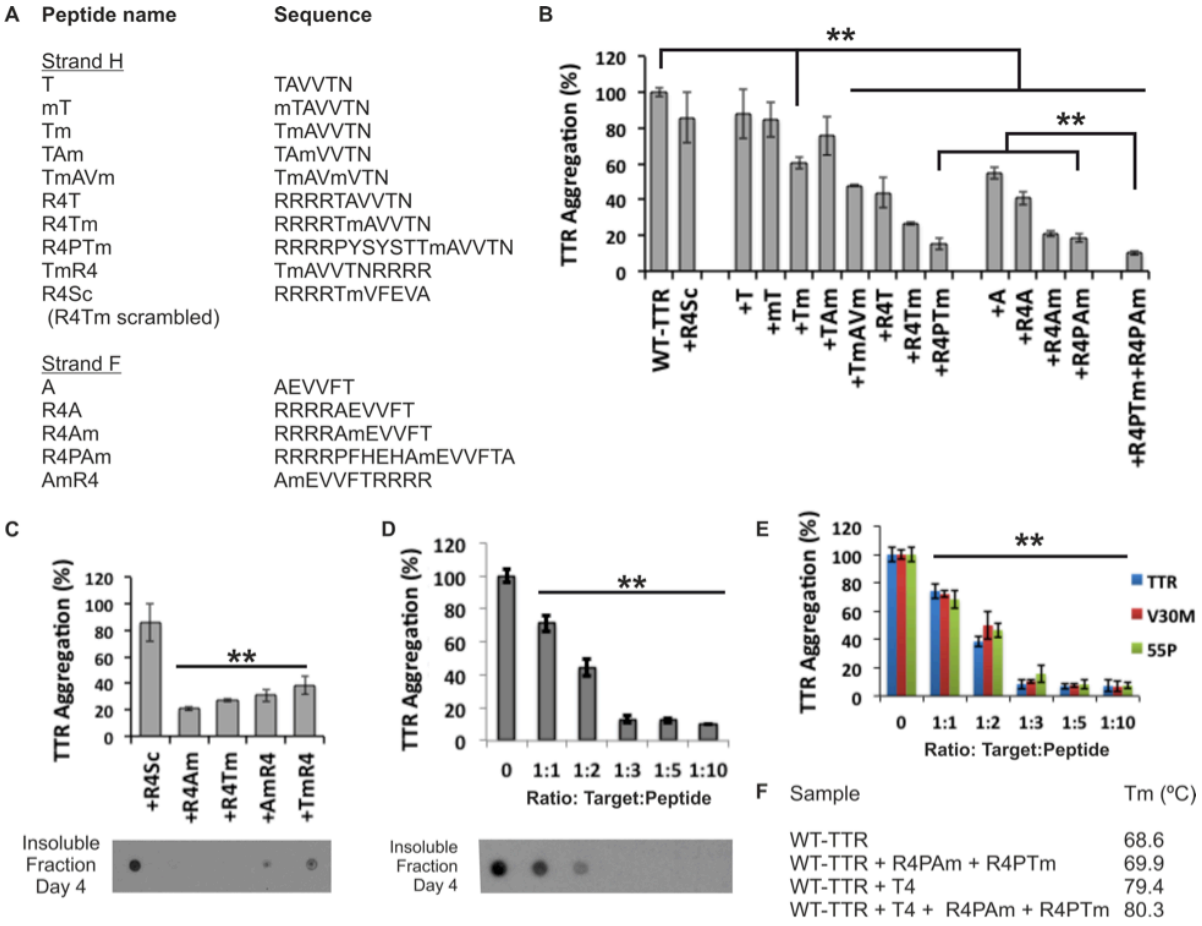

FIGURE 5. Validation of sequence-specific inhibitors ofTTR aggregation. A. List of inhibiting peptides tested. **B-E.** Evaluation of the peptide inhibitors. The histograms show the percentage of TTR aggregation after 4 days of incubation, in presence or absence of peptide inhibitor, measured by absorbance at 400 nm, with WT aggregation normalized to 100%. The initial concentration of soluble TTR was 1 mg/ml (B-D) or 3.6 μM (E). The molar ratio of peptide inhibitor compared to the concentration of the target is of 3-fold excess, unless it is labeled otherwise. Below the histograms of C and D, a His-probe dot blot shows the insoluble fraction of the samples after 4 days of incubation and solubilization with guanidinium hydrochloride. B. Initial screening of inhibitors, showing that the increase of the number of residues of the peptide, together with the addition of a charged tag and an N-methyl group in the positions predicted by the docking model (Figure 4C) significantly improved effectiveness. The two best inhibitors of TTR aggregation were found to be R4PAm and R4PAm. C. The position of the charged tag is tested. This evaluation shows that the inhibition of TTR aggregation increases when the charged tag is located at the N-terminal end. D. Dose-dependent effectiveness of the peptides R4PAm and R4PTm in combination. Observe that full inhibition of TTR

aggregation is reached when the molar ratio is of 1:3 (target:peptide) or higher. E. Aggregation assay of the familial mutants V30M and L55P in presence of R4PAm and R4PTm in combination, using a physiological concentration of protein (3.6 μM). Error bars represent SD, N=3. ** symbolizes p-value≤0.003. **F.** The midpoint temperatures of the thermal unfolding transition (Tm) of wild-type at different conditions were determined by DSC. Relative stability is compared here in presence and absence of a five-fold excess of T4 and/or the combination of R4PAm and R4PTm. TTR concentration remained 1 mg/ml. Notice that the addition of the natural ligand T4 increased the protein thermostability by 10.8º C. The addition of the peptides inhibitors increased it only by 1.3º C in absence of T4, and 0.9º C, when the ligand was present.

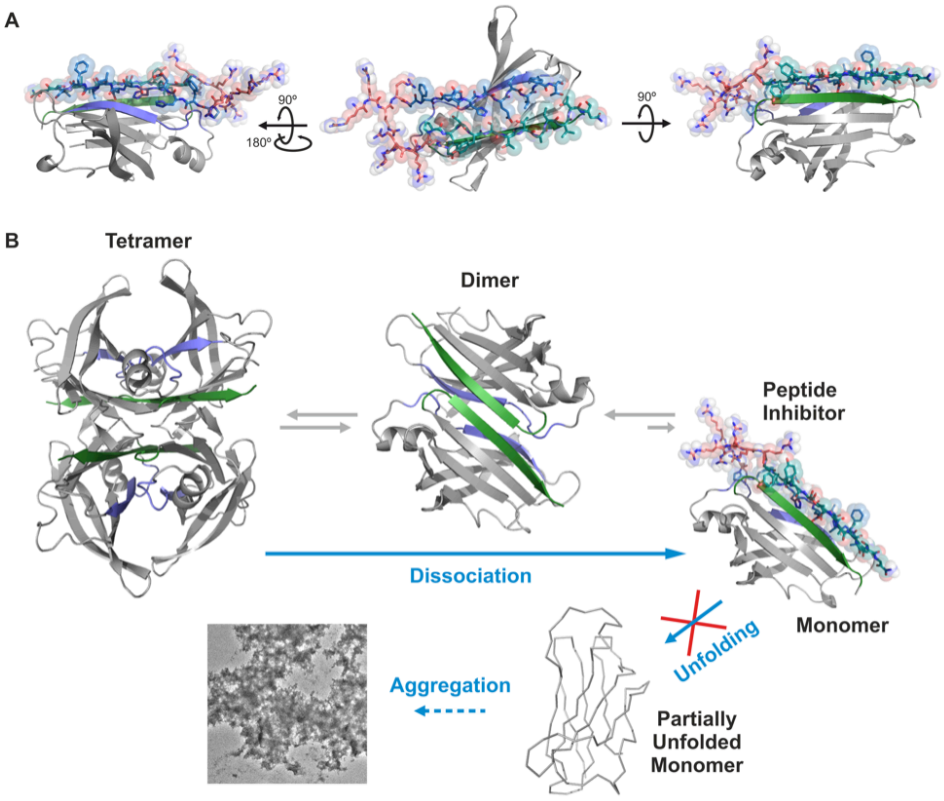

FIGURE 7. Inhibition model of TTR by the two best inhibitors of aggregation, R4PAm and R4PTm. A. Cartoon model of a monomer of TTR bound to the two best inhibitors. Peptides bind to the monomer through the self-recognition of the segments AEVVFT and TAVVTN. **B.** Model of inhibition of aggregation by peptide inhibitors. Upon dissociation of the TTR tetramer, the binding of the inhibiting peptide to the TTR monomer by self-recognition hinders

the consequent unfolding, favoring the dimerization and tetramer assembly. In this inhibition model, the hydrophobic pocket of the tetramer remains accessible for a complementary treatment with a stabilizer compound, such as tafamidis or diflunisal (Castano et al., 2012, Bulawa et al., 2012).